

wool-water system contained in a transmission horn applicator. Based on a detailed error analysis of frequency and temperature dependence of the relevant calibration curves, the operating frequency was optimized to 18 GHz in this particular case. For a variety of other materials being aspirants for industrial process control, similar developments are possible following the scopes outlined in this paper, thus opening the way for a new class of density-independent moisture meters [16].

ACKNOWLEDGMENT

The authors wish to thank G. Weidinger, who performed part of the measurements.

REFERENCES

- [1] J. B. Hasted, *Aqueous Dielectrics*. London, England: Chapman and Hall, 1973.
- [2] A. Pande, *Handbook of Moisture Determination and Control*, vols. I-IV. New York: Dekker, 1974, 1975.
- [3] W. Meyer and W. Schilz, "Microwave absorption by water in organic materials," in *Dielectric Materials, Measurements and Applications*, IEE Conf. Publ. 177. London, England, 1979, p. 215.
- [4] W. Schilz and B. Schiek, "Microwave systems for industrial measurement," *Advances Electron.*, vol. 55, p. 309, 1981.
- [5] K. Lindberg, "Microwave moisture meters in the paper and pulp industry," *Meas. Contr.*, vol. 3, p. T33, 1970.
- [6] S. O. Nelson, "Frequency and moisture dependence of the dielectric properties of red hard winter wheat," *J. Agricult. Eng. Rev.*, vol. 21, p. 181, 1976.
- [7] A. Kumar and D. G. Smith, "Microwave properties of yarns and textiles using a resonant cavity," *IEEE Trans. Instrum. Meas.*, vol. IM-26, p. 95, 1977.
- [8] M. Kent, "Microwave attenuation by frozen fish," *J. Microwave Power*, vol. 12, p. 101, 1977.
- [9] A. Klein, "Microwave moisture determination of coal-a comparison of attenuation and phase measurement," in *Proc. 10th European Microwave Conf.*, (Warsaw, Poland), p. 526, 1980.
- [10] E. M. Bstida, N. Fanelli, and E. Marelli, "Microwave instruments for moisture measurements in soils, sand and cement," in *Proc. Microwave Power Symp.* (Monaco, 1979), p. 147.
- [11] M. Tiuri and S. Heikkila, "Microwave instrument for accurate measurement of timber of sawmills," in *Proc. 9th European Microwave Conf.* (Brighton, U.K., 1979), p. 702.
- [12] S. S. Stucky and M. A. K. Hamid, "State of the art in microwave sensors for measuring non-electrical quantities," *Inst. J. Electron.*, vol. 33, p. 617, 1972.
- [13] A. Kraszewski and S. Kulinski, "An improved method of moisture content measurement and control," *IEEE Trans. Ind. Electron. Contr. Instrum.*, vol. IECI-23, p. 364, 1976.
- [14] A. Kraszewski, "A model of the dielectric properties of wheat at 9.4 GHz," *J. Microwave Power*, vol. 13, p. 293, 1978.
- [15] W. Meyer and W. Schilz, "A microwave method for density independent determination of the moisture content of solids," *J. Phys. D: Appl. Phys.*, vol. 13, p. 1823, 1980.
- [16] R. Jacobson, W. Meyer, and B. Schrage, "Density independent moisture meter at X-band," in *Proc. 10th European Microwave Conf.*, (Warsaw, Poland), p. 526, 1980.

Short Papers

The Stability of Magnetrons Under Short Pulse Conditions

B. VYSE AND H. LEVINSON

Abstract—The relationship between missing pulses, front edge jitter, and video inter-spectral noise is discussed for magnetrons operating under short pulse conditions. The measurement of missing pulse count can determine the rate of RF power growth at the start of oscillation.

INTRODUCTION

This paper is concerned with the pulse performance of a range of small, rugged magnetrons that operate in the *X*- and *Ku*-band, and have a number of special characteristics including very small size and weight, rapid switch-on, and extreme ruggedness. They

Manuscript received June 20, 1980; revised January 31, 1981. A condensed version of this paper has been presented at the 1980 IEEE-MTT International Microwave Symposium, Washington, DC.

The authors are with the M-O Valve Company, Ltd., Brook Green Works, Hammersmith, London W6 7PE, England.

have also been designed to have very good pulse stabilities, and it is the meaning and understanding of this feature that is discussed below.

Traditionally magnetron stability has been measured by the missing pulse count; a pulse is said to be missed when the energy in that pulse is less than 70 percent of the mean pulse energy. In a practical measurement the rectified RF output pulse of the magnetron is fed into an integrator which determines the mean pulse energy over a large number of pulses. Any pulse not recording 70 percent of the mean pulse energy (whether by reduced amplitude or pulselength) is counted as a missing pulse. A number of mechanisms resulting in a missed pulse are known, e.g., electrical breakdown in the device, failure to start and moding, which is oscillation in a frequency other than the dominant one. A marine radar magnetron may have a missing pulse specification of about 1 percent, the devices here are better than 0.01 percent. Clearly a missing pulse as defined above is a fairly rare event associated with an appreciable departure from the average behavior of the magnetron.

The trend in modern systems is towards higher pulse repetition



Fig. 1. Typical processed inter-spectral noise voltage (linear scale) versus time.



Fig. 2. Processed inter-spectral noise voltage similar to Fig. 1 but showing noise spikes.

rates and shorter pulselengths, and the measure of stability has become the signal-to-noise ratio of the video spectrum. Since any departure from an infinite train of perfectly uniform pulses produces spectral components between the discrete pulse-repetition frequency (PRF) components, [4] a measure of the video pulse modulation can be made by looking at inter-spectral noise. In the system considered here, the detected X-band pulse train from a magnetron is amplified in a frequency selective video amplifier, whose bandwidth is limited to half the PRF, placed between two PRF lines. (For example, if the magnetron is operating at 100-kHz PRF and 50-ns pulselength, the selective amplifier would have a bandwidth from about 1–50 kHz.) The output of the selective amplifier is further processed by rectification, to obtain a mean level. Fig. 1 shows a typical trace of the processed inter-spectral noise versus time.

Fig. 2 shows the inter-spectral noise from another valve operating under the same conditions as the valve used in Fig. 1. Both noise traces show similar dc and ac components, except that in Fig. 2 there is the occasional transient increase in the noise level (spike). Valve specifications usually place limits on both the mean and transient noise levels, since clearly both factors represent possible limitations to the sensitivity of a Doppler radar.

That some valves show spikes and some do not when operating under similar conditions has led us to look more closely at the sources of inter-spectral noise and missing pulses, and to see if any relationship exists between them. Two possible sources are front edge time jitter and frequency moding. These are discussed below.

FRONT EDGE JITTER

Magnetron pulses show detectable front edge jitter, i.e., variation from pulse to pulse of the position of the front edge of the RF pulse with respect to the time the voltage pulse reaches the threshold voltage. See Fig. 3. A time exposure photograph of the rectified RF output pulse displayed on an oscilloscope triggered from the modulator voltage shows a blurred front edge. Jitter represents a deviation from the perfect infinite pulse train and is therefore one possible source of inter-spectral noise. If sufficient care is taken in the modulator design to eliminate other possible sources of spectrum noise, e.g., ripple, or PRF modulation, it is found that jitter remains as a detectable residual source of noise. There is strong experimental and theoretical evidence that this jitter is the cause of the dc component of noise in Figs. 1 and 2.

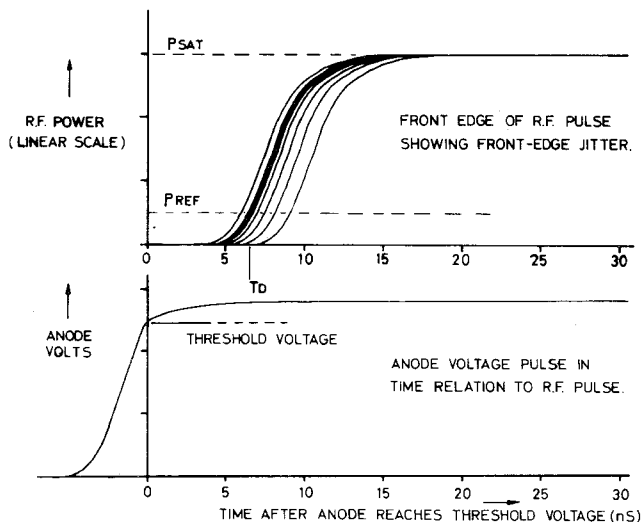


Fig. 3. Front edge of detected RF pulse, showing front edge jitter and time relationship with anode voltage pulse.

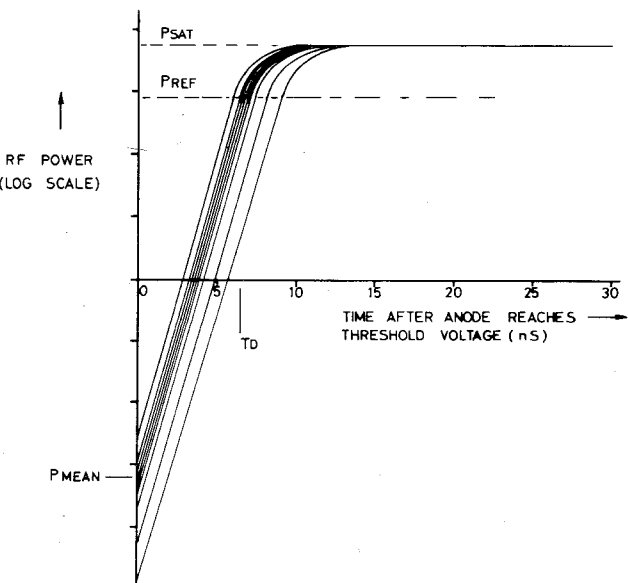


Fig. 4. Front edge of detected RF pulse plotted on a logarithmic scale and showing exponential growth of power from starting noise.

CALCULATION OF VIDEO SPECTRUM OF RECTIFIED RF PULSETRAINS WITH JITTER

Macfarlane [4] gives the following expression for the spectral energy density $R(\omega)$ of a pulsetrain under random modulation:

$$R(\omega) = \frac{1}{T} \left(\overline{(A - \bar{A})^2} + \frac{2\pi}{T} \delta \left(\frac{\omega - 2n\pi}{T} \right) (\bar{A})^2 \right)$$

where

$$\bar{A} = \int_{-\infty}^{+\infty} G(\omega, x) q(x) dx$$

$$\overline{(A - \bar{A})^2} = \int_{-\infty}^{+\infty} G^2(\omega, x) q(x) dx - (\bar{A})^2$$

$G(\omega, x)$ is the spectrum of a single pulse of unit amplitude occurring at zero time with one of its parameters modified by the quantity x , and $q(x)$ is the distribution function, i.e., the probability that the quantity x lies between x and $x+dx$ is $q(x)dx$. In general, the spectrum consists of a line spectrum containing the δ term with energy $(2\pi/T^2)(\bar{A})^2$ and a continuous spectrum with spectral energy density

$$\frac{1}{T} \overline{(A - \bar{A})^2}.$$

The comparison of spectrum envelope shapes which characterise various types of pulse modulation has been published elsewhere [2]. Front edge jitter may be considered as partly pulselength and partly inter-pulse time jitter and creates a continuous uniform background of noise unlike other modulations which have zero noise regions of the spectrum.

In general the amplitude of the noise spectrum depends upon the particular probability function of the modulation. In practice, the amplitude of the spectral noise is very nearly the same for all distributions with the same standard deviation σ . For small ω , the case of practical importance, this is strictly true. For such a case, with a rectangular pulselength $\xi + x$, with fixed back edge and variable front edge standard deviation σ , $PRF(1/T)$

$$\bar{A} = \frac{\xi}{\sqrt{2\pi}} \frac{\sin \frac{\omega\xi}{2}}{\omega\xi} \text{ and } \overline{(A - \bar{A})^2} = \frac{\sigma^2}{2\pi}.$$

The result is fortunate because we have been unable to treat analytically the case of special interest discussed in a following section because the particular distribution is too complicated. Hence the signal-to-noise ratio, S/N , measured into a bandwidth B is given by

$$S/N = 2\pi\xi^2/\sigma^2 TB.$$

For the particular pulse condition mentioned in the introduction, i.e., 100 kHz PRF ($1/T$) and 50-ns pulselength (ξ), a typical front edge jitter with standard deviation σ of about 1 ns would produce a S/N ratio measured into a 50-kHz bandwidth of 45 dB. This accords well with observations.

THE EXPERIMENTAL VERIFICATION OF RELATIONSHIP BETWEEN JITTER AND INTER-SPECTRAL NOISE

The investigation of video inter-spectral noise requires a modulator system which is sufficiently stable with regard to PRF, pulselength, and amplitude modulation that it produces a noise level well below that due to the magnetron itself. This can be achieved by relatively conventional means but for the present

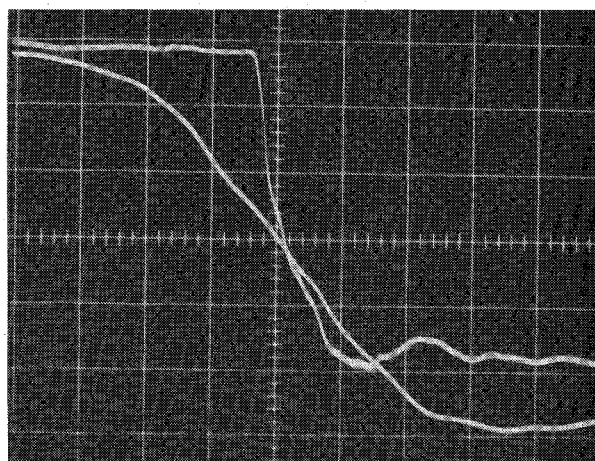


Fig. 5. Front edge of voltage pulse with and without the spark gap: Horizontal scale: 2 ns/division; Vertical scale: 90 V/division.

purpose a fast rise pulse derived from a low impedance source is also required so that the magnetron jitter can be investigated under well-defined voltage conditions. For noise measurements a PRF of about 10 kHz and short pulselength (<20 ns) are required. The system chosen to pulse the 800-V X-band valve MAG17 was a line type modulator with a 50Ω delay line and CV4112 thyratron switch (miniature version of 3C45). The low output impedance (25Ω) was achieved by means of a parallel 50Ω load. The pulselength was determined by the length of the delay line, and adequate ht smoothing produced the required amplitude stability. The required PRF stability (less than 5.0 ns of jitter) was achieved using an EH pulse generator driving a pulse amplifier which applied a large rapid pulse to the thyratron grid. Great care was taken in the construction of the modulator to achieve the fastest possible pulse. The best performance was 5–6 ns, 10–90-percent rise time, and under these conditions the magnetron-modulator system worked well up to a PRF of 20 kHz. An improvement in the 10–90-percent voltage rise time to 2 ns was achieved, with only a tolerable loss of convenience and without loss of stability, by means of a coaxial spark gap in series with the pulse. The effect of the gap is to clip off the slow lower edge of the thyratron pulse as shown in Fig. 5. The spark gap used nitrogen at reduced pressure and consisted of 0.5-mm tungsten rods mounted coaxially and encapsulated in series with a 50Ω line from the thyratron. The gap was adjustable being typically 0.25 mm.

The video spectrum from a crystal detector was displayed using a Rohde and Schwarz audio frequency spectrograph. An example of the analysis is shown in Fig. 6. The analyzer has a 20-kHz swept bandwidth with a dynamic range of 80 dB and a filter bandwidth of either 10 Hz or 200 Hz at the 3-dB points. In order to obtain a reasonable S/N ratio the PRF must not be too high (less than 10 kHz) and the pulselength very short (perhaps 10 ns). Also, to obtain maximum deflection on the most sensitive range, with the 0.5 V or so which can be obtained from the crystal detector it was necessary to use a low-pass, low-noise amplifier.

Measurement of video inter-spectral noise of the MAG17 magnetron on an existing stable conventional modulator suggested a front edge jitter of about 2.0 ns. Measurement of jitter itself by means of a photo-densitometer analysis of a time exposure photograph confirmed this figure. The use of the fast rise

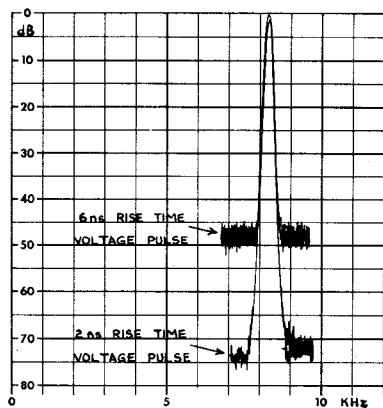
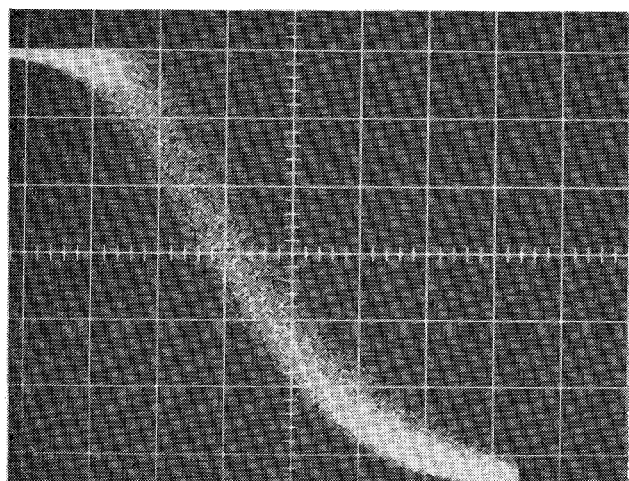
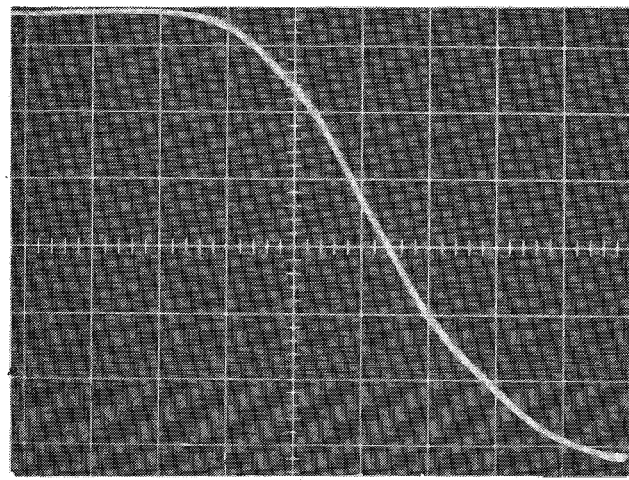


Fig. 6. Video noise spectra, showing reduction of the noise when the rise time of the voltage pulse is reduced from 6 to 2 ns.



(a)



(b)

Fig. 7. Front edge of rectified RF pulse showing front edge jitter: Horizontal scale: 1 ns/division. (a) Rise time of voltage pulse: 6 ns. (b) Rise time of voltage pulse: 2 ns.

stable thyratron modulator described above and with a rise time of about 6 ns, showed very similar figures for a number of valves both from noise measurements and through direct measurements of jitter. With the series spark gap and a 2-ns rise time the jitter

improved by more than a factor of ten, see Fig. 7, and the video inter-line noise improved accordingly, see Fig. 6. We have, therefore, a direct quantitative observation of the relationship between jitter and video inter-line noise.

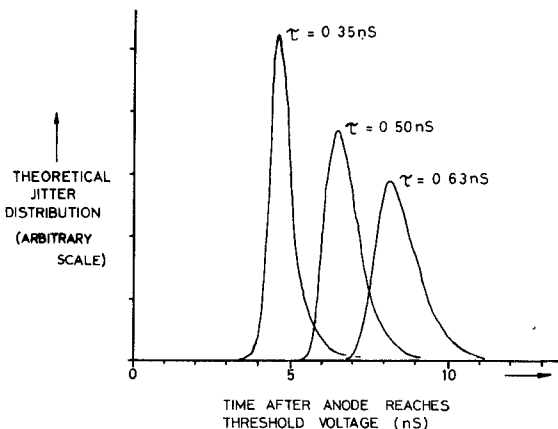


Fig. 8. Theoretical jitter distributions for three values of τ but same $P_{\text{ref}}/P_{\text{mean}}$.

THE PROBABILITY DISTRIBUTION OF FRONT EDGE JITTER

Observation of the RF power growth at the start of oscillation under constant voltage conditions indicates exponential growth over typically 45 dB up to the level of saturation [1], [2], [5]. All exponentially growing systems must start from a finite amplitude if they are to build up to a given amplitude in a finite time. In the case of the magnetron the starting level is generated by the noise modulation of the crossed-field electron beam. Since the dominant resonance (π -mode) of the anode circuit has a high Q , the response of the anode circuit to the broad-band noisy electron beam when threshold voltage is reached is a rapidly growing quasi-sinewave. The initial transients rapidly die away leaving the exponentially growing wave of frequency close to the π -mode characteristic of the linear interaction between beam and circuit wave. The RF voltage on the circuit has an amplitude which can be described as

$$v = R \exp(bt)$$

where b is the RF voltage growth constant. R is the apparent amplitude of the RF voltage on the circuit at time zero, i.e., when threshold voltage is attained. Since R is noise generated, its amplitude will vary from pulse to pulse. If the noise is purely random R will fluctuate in a precisely known statistical manner [6], i.e., it will have a Rayleigh probability distribution. The higher the amplitude of this starting signal, the sooner a reference power level P_{ref} is reached, Fig. 4. The jitter probability, i.e., the probability that this reference level is reached in the time interval t to $t+dt$ from starting, i.e., from when the threshold voltage is reached, is given by [1]

$$f(t)dt = \frac{P_{\text{ref}}}{\tau P_{\text{mean}}} \cdot \exp\left(-\frac{t}{\tau}\right) \cdot \exp\left(-\frac{P_{\text{ref}}}{P_{\text{mean}}} \cdot \exp - \frac{t}{\tau}\right) \cdot dt \quad (1)$$

where τ is the RF power growth constant defined by

$$P(t_2) = P(t_1) \exp\left(\frac{t_2 - t_1}{\tau}\right)$$

and P_{mean} is the average noise power on the RF circuit when $t=0$.

Some probability distributions for $\tau=0.35$, 0.50, and 0.63 ns are shown in Fig. 8. It can be shown that the width of the distribution is 2.45τ between the half probability and 4.86τ between the 10-percent probability points and might be typically 1–2 ns.

These theoretical front edge jitter distributions have been compared with observed distributions measured from photo-densi-

tometer analysis of time exposure photographs and show very close agreement [1], [3] in practical cases where the rise time of the modulator voltage pulse is more than about 6 ns.

PROBABILITY DISTRIBUTION OF ANOMALOUS JITTER

As mentioned in a previous section anomalous results are observed under very rapid rate of voltage rise and much reduced jitter is observed; at least an order less than that predicted by random noise theory or observed on slower rates of voltage rise. In previous work [1], [3], [5], a controlled method of varying the prethreshold excitation time T_p is discussed and indeed finds that as T_p increases, jitter increases smoothly from low to high values. This method was used in conjunction with the photodensitometer measurements to investigate the jitter distribution of the MAG17 magnetron for a range of T_p values. Since T_p can be varied without changing the operating voltage, the rate of RF growth may be kept constant as T_p varies. A series of measured distributions corresponding to a range of T_p for the same τ value are shown in Fig. 10. It will be seen that for very short T_p the measured distribution is narrower, appears earlier in time and is more symmetrical. These characteristics are precisely as predicted for random noise with superimposed sinewave, [1], [6]. In this case the jitter probability distribution is given by

$$P_r(t)dt = \frac{P}{\tau(P_{\text{mean}} - E^2/2)} \exp\left[-(P + E^2/2)/(P_{\text{mean}} - E^2/2)\right] \cdot I_0\left(\frac{\sqrt{2P}E}{P_{\text{mean}} - E^2/2}dt\right)$$

where $P = P_{\text{ref}} \exp(-t/\tau)$, E is the amplitude of the sinusoidal component, I_0 is a Bessel function.

The probability distribution is plotted in Fig. 9 for several values of $E^2/2$ with the same noise power in each case.

All the evidence is consistent with the hypothesis that for very rapid voltage rise the space charge has a sinusoidal modulation impressed upon it, over and above the random noise modulation, which becomes synchronous with the circuit wave at threshold voltage. The facts are also consistent with the hypothesis that the amplitude of the sinewave declines over a period of time, the noise component remaining unchanged, finally becoming negligible in 10 or 15 ns as witnessed by the comparison between Figs. 9 and 10. This then is the explanation held out for reduced jitter.

After careful elimination of other possible explanations for this phenomena it is concluded that for very rapid rates of voltage rise

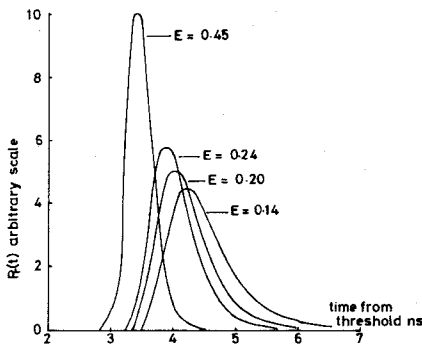


Fig. 9. Theoretical jitter distributions corresponding to random starting noise with superimposed sinewave of various amplitudes. $\tau = 0.5$ ns.

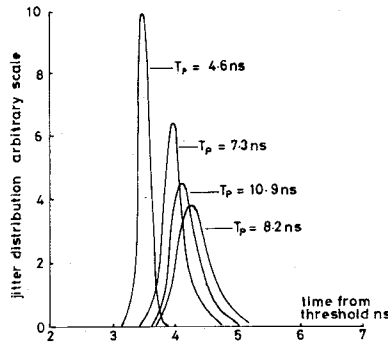


Fig. 10. Measured jitter distributions as a function of T_p . MAG17 $\tau = 0.35$ ns.

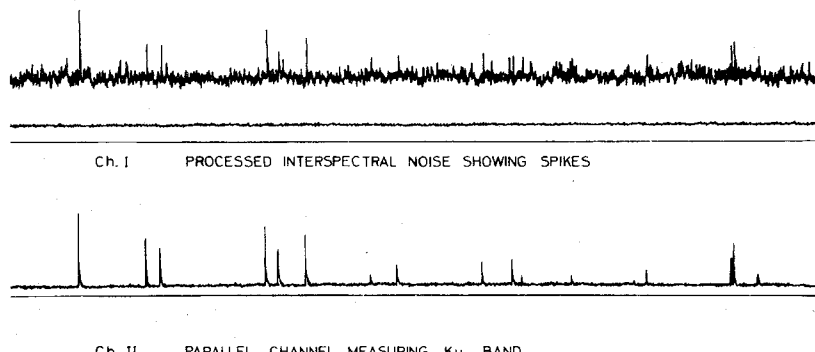


Fig. 11. Channel I. Processed inter-spectral noise voltage similar to Fig. 2. Channel II. Inter-spectral noise voltage measured simultaneously with Channel I but through Ku-band high-pass filter.

there is a sinusoidal current impressed upon the beam. The suggestion is made that this is due to the segmented nature of the anode. Electrons are not initially drawn off uniformly around the cathode but in plumes corresponding to the anode segments. It is also suggested that this imposed periodicity persists for a few nanoseconds (circuits of the cathode) before space charge effects finally smooth out the ripple. It is the decay of this ripple with increasing T_p which causes the jitter to increase with T_p in the manner described.

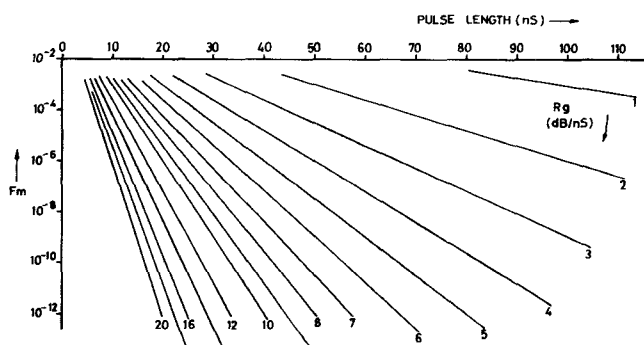
MODING

The theories put forward for starting and jitter in the dominant π -mode apply equally well for oscillation in any of the other possible modes of oscillation of the magnetron, except that the design has been made very much to favour oscillation in the

π -mode. Nevertheless, there remains theoretically the statistical possibility that starting noise will occasionally favor oscillation in a mode other than the π -mode, i.e., moding may take place.

To investigate the effect of moding on the inter-line noise, the noise was measured on two channels simultaneously. Typical outputs are shown in Fig. 11. The first channel is similar to Figs. 1 and 2 whereas the microwave detector for the second channel was preceded by a 13-GHz high-pass filter giving ≥ 50 -dB isolation at the valve operating frequency (~ 10 GHz).

The only significant output from the Ku-band noise channel, Ch II, was the occasional spike—most of which corresponded with spikes in the normal measurement channel, Ch I. A check with a microwave bandpass filter showed the Ku-band signal to be between 14 and 16 GHz, which includes the most probable moding frequency, i.e., spikes are caused by moding. The lack of

Fig. 12. Probability (F_m) of a missed pulse versus pulselength.

any significant mean level from the *Ku*-band noise channel implies that, in this case, moding was not making a significant contribution to the mean inter-spectral noise level.

FRONT EDGE JITTER AND MISSED PULSES

From the jitter distributions shown in Fig. 8, it can be seen that the probability of a late pulse decreases rapidly with time. However, occasionally a pulse will be late by 30 percent or more of the mean pulse duration and this would register as a missing pulse as defined in the introduction. Integration of (1) above shows that the probability $F(t)$ that a pulse will reach the reference level after time t asymptotically becomes,

$$\log_{10} F(t) = -\frac{(t - T_D)}{10} \cdot R_g$$

where R_g , the RF growth rate, is given by

$$R_g = \frac{4.34}{\tau} \text{ dB/ns}$$

and T_D , the delay time, is given by

$$\exp \frac{T_D}{\tau} = \frac{P_{\text{ref}}}{P_{\text{mean}}}.$$

Physically T_D is the time required for the most probable power growth curve to reach the reference level.

Now, assuming the mean starting time is equal to T_D , a missed pulse will occur when

$$t - T_D \geq 0.3 T_p$$

where T_p is the pulselength, so the probability of a missed pulse, caused by front edge jitter only, is given by

$$\log_{10} F_m = -0.03 \cdot R_g \cdot T_p. \quad (2)$$

Plots of F_m versus T_p , for different R_g , are shown in Fig. 12, and it can be seen that the probability of jitter causing a missed pulse decreases very rapidly with increasing pulselength and RF growth rate. Note the missed pulse rate is given by F_m multiplied by the PRF.

It is interesting to note from the above that digital measurement of the missing pulse count on short pulse conventional modulators gives information about the rate of RF growth of the magnetron.

CONCLUSIONS

Front edge jitter is a major source of mean inter-spectral noise, it is fundamental to the starting of a magnetron and depends on the rate of RF growth only. For very rapid rate of rise of the

modulation pulse, jitter may be anomalously low.

In the increasingly more common case of very short pulses, or when the RF growth rate is very low, front edge jitter can result in "traditional" missing pulses (≤ 70 -percent mean energy).

Transient increases in the inter-line noise (spikes) can be caused by the magnetron operating in the wrong mode.

Specifications calling up low levels of mean inter-line noise imply small front edge jitter and, therefore, virtually no missing pulses.

In a system in which front edge jitter is the only source of instability, a measurement of the missing pulse count could, together with (2), be used to calculate the rate of RF growth.

REFERENCES

- [1] B. Vyse, "Jitter and the growth of RF oscillation in pulsed magnetrons," Ph.D. dissertation, Edinburgh, 1971.
- [2] B. Vyse and M. A. Hulley, "Growth processes and inter-line noise in pulsed magnetrons," in *Proc. 7th Int. Conf. Microwave and Optical Generation and Amplification*, Hamburg, 1968.
- [3] M. A. Hulley and B. Vyse, "A mathematical model of RF build-up and inter-line noise in pulsed magnetrons," in *Proc. 8th Int. Conf. on Microwave and Optical Generation and Amplification*, Holland, 1970.
- [4] G. G. Macfarlane, "On the energy spectrum of an almost periodic succession of pulses," *Proc. IRE*, vol. 30, p. 1139, 1949.
- [5] M. A. Hulley and B. Vyse, "The investigation of pulsed magnetron performance at X-band with voltage rise times in the nanosecond region," in *Proc. 6th Int. Conf. Microwave and Optical Generation and Amplification*, Cambridge, 1966.
- [6] S. O. Rice, "Mathematical analysis of random noise," *Bell Syst. Tech. J.*, vol. 24, part III, p. 100, 1945.

Guided Magnetostatic Waves of the YIG Plate Magnetized Nonuniformly

KEN'ICHIRO YASHIRO AND SUMIO OHKAWA

Abstract— It is shown that magnetostatic waves may propagate along a discontinuity of the internal dc magnetic field when its strength is made nonuniform such as a step. Backward waves may also propagate in this magnetic field configuration.

In the past, the effects of nonuniformity of the internal dc magnetic field on the generation or propagation characteristics of magnetostatic modes have been discussed by a number of investigators [1]–[6]. Recently, it has been reported [7] that controlled magnetostatic waves can propagate in desired frequency ranges at desired speed if appropriate dc magnetic field gradients are applied. In this work, we study magnetostatic wave propagation for the case in which the dc magnetic field in the inner region of the sample is stronger or weaker than the field in the outer region.

The external static field shall be applied by using pole pieces such that the internal magnetic field is deliberately nonuniform. Then, which modes may propagate in the structure shown in Fig.

Manuscript received October 28, 1980; revised January 29, 1981.

The authors are with the Department of Electronic Engineering, Faculty of Engineering, Chiba University, Chiba, 260 Japan.